ELSEVIER

Polymer 44 (2003) 2553–2562

polymer

www.elsevier.com/locate/polymer

Crystallization and thermoelectric behavior of conductive-filler-filled poly(ε-caprolactone)/poly(vinyl butyral)/montmorillonite nanocomposites

Tzong-Ming Wu*, Jen-Chih Cheng, Ming-Chih Yan

Department of Material Science and Engineering, National Chung Hsing University, 250 Kuo Kuang Road, 402 Taichung, Taiwan, ROC

Received 17 September 2002; received in revised form 6 December 2002; accepted 15 January 2003

Abstract

Crystallization and thermoelectric properties of poly(ε-caprolactone) (PCL)/poly(vinyl butyral) (PVB)/montmorillonite (MMT) nanocomposites containing carbon black (CB) have been studied as a functions of a small amount of amorphous PVB content and a wide range of molecular weight of PVB. X-ray diffraction data of PCL/PVB/MMT nanocomposites indicates most of the swellable silicate layers are exfoliated and randomly dispersed into PCL/PVB system. The band spacings of PCL spherulites in PCL/PVB/MMT nanocomposites decrease with increasing PVB content, and this indicates that increasing the PVB content greatly shortens the period of lamellar twisting. The presence of 1 wt% MMT and higher molecular weight of PVB also shorten the period of PCL lamellar twisting. Nucleation and crystallization parameters, such as growth rate G and Avrami exponent n, can be determined by using POM and DSC isothermally crystallized at 41 °C. For samples with the same CB content, the intensity of positive temperature coefficient (PTC) (I_{PTC}, defined as the ratio of peak resistivity to resistivity at room temperature) of the nanocomposites was increased as the content and the molecular weight of PVB increases. The change of the PTC property related to the morphological difference (i.e. period of lamellar twisting) in the nanocomposites can be discussed.

Keywords: Nanocomposite; Positive temperature coefficient; Poly(ε-caprolactone)

1. Introduction

Conductive polymer composites can be used in the area of self-regulating heater, current protection devices, micro-switches sensors and electromagnetic interference shields. The conventional method of preparing conductive polymer composites is to disperse a conductive filler such as carbon black (CB), carbon fiber, graphite and metal foil, throughout the polymer matrix. The conductivity of CB-filled polymer depends not only on the properties of CB such as particle size, concentration, dispersion state and aggregate shape, but also the characteristics of polymer matrix such as chemical structure, morphology, crystallinity and processing conditions [1–10]. A crystalline polymer filled with critical amount of CB shows a sharp increase in electric resistance with the temperature around melting temperature (T_m) of the crystalline polymer, which is called positive temperature coefficient (PTC).

During the last few decades, the PTC phenomenon has attracted much interest and studies [11–15]. Although there is no satisfactory theory to explain the PTC phenomenon, there have been many models such as thermal expansion [11], electron tunneling [12,13], double percolation [9,14–17], thermal fluctuation-induced tunneling [18] and cooperative effect of changes in crystallinity and volume expansion [7] to elucidating its specific aspects. All of these models suggest that the volume expansion plays an important role in the PTC behavior, but the explanation based on the tunneling effect is widely accepted. According to this mechanism, electrons pass through the thin gaps between adjacent CB particles, aggregates and agglomerates at a practical magnitude of the electrical field. The gap width could dominate the electrical properties since the current is an exponential function of the gap width.

On the other hand, the effect of polymer morphology and

* Corresponding author. Tel.: +886-4-22840500x806; fax: +886-4-22857017.
E-mail address: tmwu@dragon.nchu.edu.tw (T.M. Wu).

0032-3861/03/$ - see front matter © 2003 Elsevier Science Ltd. All rights reserved.
doi:10.1016/S0032-3861(03)00106-X

crystallinity on the thermoelectric properties of CB-filled polymer composites was based on the percolation theory [14–17]. Additional critical amount of CB is necessary to build up continuous conductive network referred as the percolation threshold. In this case, CB particles aggregates and agglomerates are localized either at the interface of co-continuous phase of two polymers or in the continuous phase of only one polymer. Therefore the conductivity of CB-filled polymer composites is sensitively influenced by their relative morphology and crystallization behavior. From this point of view, there is a very interesting polymer system, poly(ε-caprolactone) (PCL)/poly(vinyl butyral) (PVB) [19], where the nucleation frequency of crystalline PCL spherulites is strikingly reduced by adding only up to several percent of amorphous PVB. Only 1% addition of PVB can dramatically reduce the nucleation density and allow the spherulites of PCL to grow on the order of centimeters. These morphological changes are also significant enhancement in the regularity of the twisted lamellar in the banded PCL spherulites. Therefore PCL/PVB systems are suitable for studying the effect of morphological changes on the PTC properties due to remarkable change in their crystalline morphology [20,21].

Polymer nanocomposites defined by the particle size of the dispersed phase containing at least one dimension less than 100 nm have relatively high aspect ratio and attract much interest due to their excellent mechanical, physical and thermal properties [22–25]. Typical preparation of synthesizing polymer nanocomposites is either intercalation of a suitable monomer and then exfoliating the layered silicate host into their nanoscale elements by subsequent polymerization or direct insertion of polymer chains from melt or solution state by using a conventional polymer process. The high aspect ratio of layered silicate would affect the physical and mechanical properties of the synthesizing polymer nanocomposites. In this study, the polymer nanocomposites containing crystalline/amorphous polymers and CB has been used to prepare the CB-filled polymer nanocomposite. The morphology of crystalline/amorphous polymer nanocomposites with no ingredients has been developed, which is greatly influenced by the interaction of the crystalline/amorphous polymers. However, there is no extensive investigation on the crystallization and morphology of polymer nanocomposites containing conductive fillers, especially CB. The difficulty of this investigation is attributable to the fact that the presence of CB could hinder the microscopic observation during the crystallization process.

In this report, we have used swellable layered montmorillonite (MMT) interacted with CB as the dispersed phase to prepare CB-filled PCL/PVB/MMT nanocomposites. The effect of nano-scale MMT and a wide range of molecular weight of PVB on the morphology, crystallization behavior and thermoelectric properties of PCL/PVB polymer nanocomposites have been investigated.

2. Experimental

2.1. Specimens

The PCL and PVB with various molecular weight used in this study were purchased from Polysciences Inc. The weight-average molecular weight (Mw) of PCL, PVB1, PVB2 and PVB3 is 65,000, 48,000, 110,000 and 145,000, respectively. The natural sodium MMT with a trioctahedral smectite structure and a cation exchange capacity (CEC) of 110 mequiv./100 g was used as the dispersed phase to improve the distribution of CB. The used CB was Vulcan XC-72 (N_2 surface area = 254 m^2/g; DBP oil absorption = 174 cm^3/100 g; mean particle diameter = 30 nm) produced by the Cabot Corporation. The surface of natural sodium MMT was modified by cationic exchange between Na^+ in MMT galleries and *n*-hexadecyl trimethyl-ammonium bromide cations (CTAB) in an aqueous solution at 60 °C for 2 h and then mixed with the solution of CB. The 1 wt% treated MMT with CB was then added into pre-mixing PCL/PVB solution, mixed for 2 h and dried in vacuum oven at 45 °C for 2 h.

2.2. Wide angle X-ray diffraction

X-ray $\theta/2\theta$ diffraction scans of these specimens were obtained using a 3kW Rigaku III diffractometer equipped with Ni-filtered Cu Kα radiation. These data were recorded in the reflection mode. The degree of crystallinity of PCL/PVB/MMT nanocomposites was calculated from the integrated area of X-ray diffraction data, for which we assumed Gaussian profiles for crystalline and amorphous peaks.

2.3. Thermal analysis

Thermal analysis of the samples was preformed using a Perkin–Elmer PYRIS Diamond differential scanning calorimeter (DSC) calibrated using indium and all experiments were carried out under a nitrogen atmosphere. All specimens were weighted in the range of 6–7 mg. The crystallization temperature (T_c), exothermic heat of crystallization (ΔH_c), crystalline melting temperature (T_m), and heat of fusion of polymer crystalline (ΔH_m) were obtained by the following procedures: these specimens were heated to 80 °C at a rate of 100 °C/min and held for 5 min to remove the residual crystals, which may be seeds for the following crystallization. The samples were then quenched to 0 °C and heated to 80 °C at a rate of 10 °C/min.

For isothermal crystallization, the specimens were also heated to 80 °C at a rate of 100 °C/min and held for 5 min to remove the residual crystals, then they were quickly cooled to 41 °C. Heat fusion versus time for isothermal crystallization (ΔH_c) was recorded. The specimens isothermally crystallized at 41 °C were heated to 80 °C at a rate of 10 °C/min.

2.4. Polarized optical microscopy (POM)

Optical microscopy was carried out by using Zeiss optical microscope equipped with a Mettler FP-82 hot stage and crossed polarizers. The crystallization process was examined using the following temperature sequence. The material was heated to melt at 80 °C for 20 min on the hot stage to remove previous thermal history and then quenched to 41 °C for isothermal crystallization. Optical microscopy was recorded at 41 °C for various times. The density of nuclei was evaluated by counting the number of spherulite in each photograph per section area.

2.5. Electrical properties

The sample of nanocomposites was cast on the surface of glass plates and then the silver paste was painted on each end of the sample surface to ensure electrical contact with the electrodes. The species were treated at 45 °C for 30 min and then cooled in air to room temperature. The thickness of thin film was in the range of ~0.15 mm. The temperature-resistivity curves of nanocomposites heated at a rate of 1 °C/min to 70 °C during resistivity measurement were measured by a digital multimeter (SM-823, TOA). Each data shown here is the mean value of the measurement from at least three samples.

3. Results and discussion

Fig. 1 shows X-ray diffraction data of neat layered MMT, CTAB-modified MMT, PCL/MMT and 5 wt% PVB2 in PCL/PVB2/MMT and PCL/PVB2/MMT/CB nanocomposites. From the peak position (d_{001}-reflection) of X-ray diffraction data, the interlayer distances of the MMT can be calculated. The d_{001}-reflection for the neat MMT (trace a in Fig. 1) was found at a $2\theta \approx 7.14°$, corresponding to an interlayer distance of 12.4 Å. Further surface modification by CTAB cations shifts the X-ray data into smaller angles and substantially increases interlayer distances. The d_{001}-reflection of CTAB-modified MMT (trace b in Fig. 1) was found at $2\theta \approx 2.3°$, which corresponds to an interlayer distance of 38.4 Å. Effect of surface modification on the interlayer distance provides reasonable space for the dispersion of conductive particles and polymer chains. Therefore CTAB-modified MMT could probably use as the media of dispersion for the intercalation of CB particles and PCL/PVB2 polymer chains. All X-ray diffraction data (traces c, d and e in Fig. 1) of solution intercalation of PCL/PVB2 into CTAB-modified MMT with or without CB showed no d_{001}-reflection in the relevant region, thus indicating the interlayer distances of layered silicate are larger than 48 Å and PCL/PVB2 are well exfoliated into the swellable layered silicate with or without CB. Similar X-ray data are also obtained for PCL/PVB1/MMT and PCL/PVB3/MMT systems. Therefore the dispersion of PCL/PVB/MMT nanocomposites is highly exfoliated and is independent of the molecular weight of PVB.

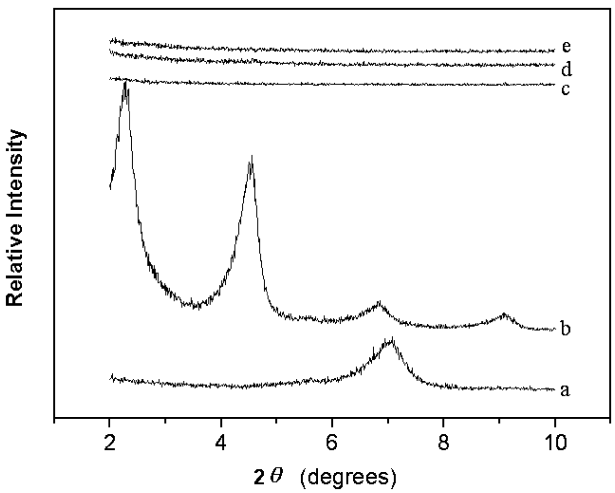

Fig. 1. X-ray diffraction data of (a) neat layered MMT, (b) CTAB-modified MMT, (c) PCL/MMT, (d) 5 wt% PVB2 in PCL/PVB2/MMT nanocomposites and (e) 5 wt% PVB2 in PCL/PVB2/CB/MMT nanocomposites.

Fig. 2 shows the POM of various PVB2 content in PCL/PVB2 and PCL/PVB2/MMT systems crystallized at 41 °C. When pure PCL was crystallized from the melt, the grown spherulites show typical extinction crosses under the polarizing microscopy. By adding 1 wt% amorphous PVB2 into PCL, larger spherulites can be observed due to the decreasing nucleation density in PCL with the presence of small amount of PVB2. The addition of more PVB2 into PCL up to 5–10 wt%, the nucleation density in PCL further decreases and the specimens can be stored for at least 20 min at 41 °C without nucleation occurring at all. The spherulites grown in PCL/PVB2 system also show banding structure with radial separations in the range of ~20 μm. The occurrence of banding structure in PCL spherulites is attributable to a twisting of crystallographic orientation about radii that probably reflects cooperative twisting of radiating lamellar crystals about their axes of fastest growth. This result implies a high degree of coordination in the packing of lamellae within fairly compact structure and is significant effectiveness in suppressing primary nucleation of PCL spherulites. Once crystalline PCL nucleated, spherulites in PCL/PVB2 grow at radial rates comparable in order of magnitude to those observed in pure PCL at the same temperature. The band spacings are decreased with increasing PVB2 content, and this indicates that increasing the PVB2 content shortens the period of lamellar twisting. However, the spacings varied from place to place even in the same spherulite, and quantitative comparison was unfeasible. Addition of CB into 5 wt% PVB2 in PCL/PVB2 system, the growing boundary of spherulites is almost impossible to distinguish from each other due to the poor visual field with CB. However, the larger spherulite with a Maltese cross was observed even though the poor illustration with CB in the melt and in the spherulite. The

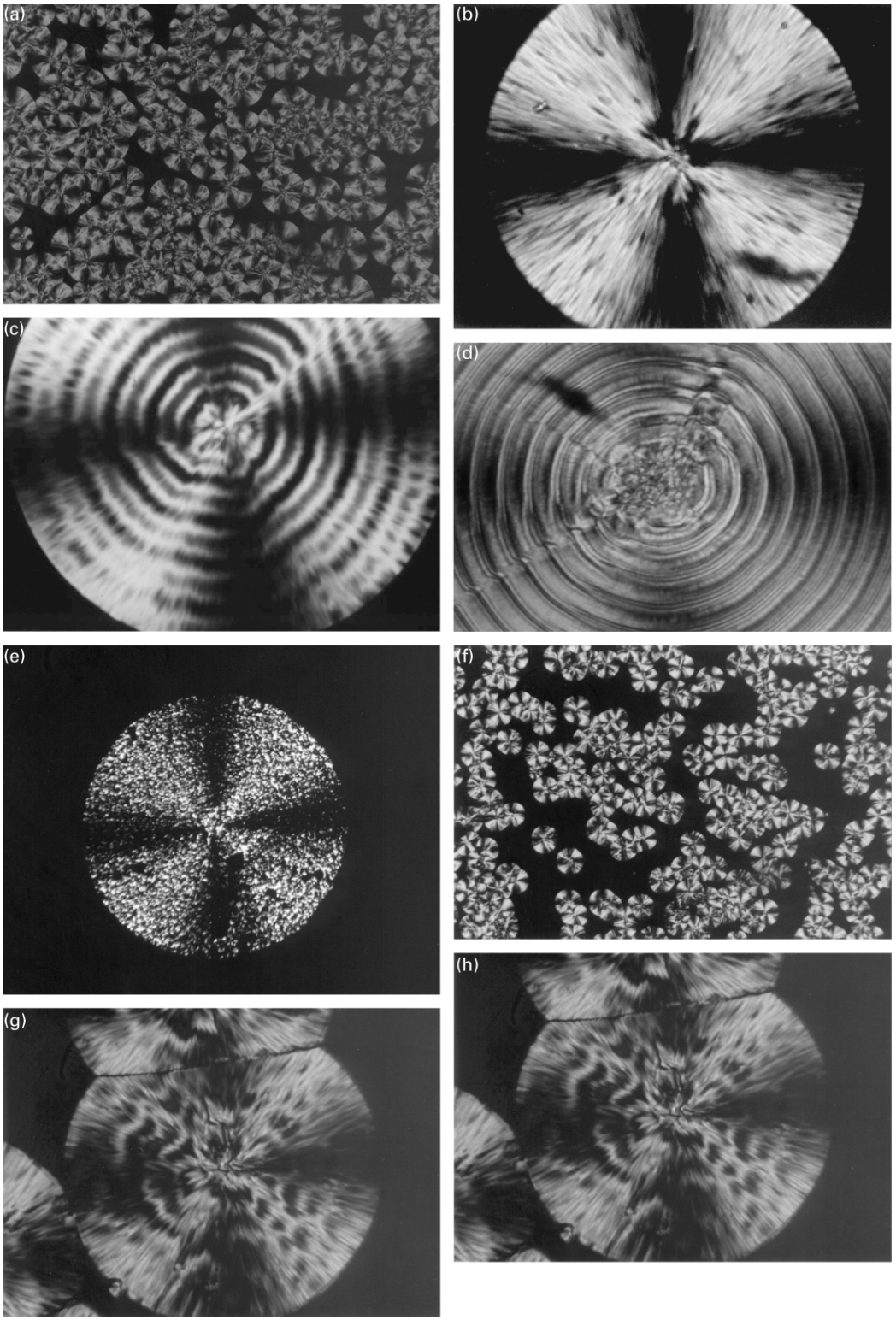

Fig. 2. Cross-polarized optical micrographs describing the extinction rings of (a) pure PCL, (b) 1 wt% PVB2 in PCL/PVB2, (c) 5 wt% PVB2 in PCL/PVB2 and 10 wt% PVB2 in PCL/PVB2 spherulites without CB crystallized at 41 °C, (e) Cross-polarized optical micrographs of 5 wt% PVB2 in PCL/PVB2 with CB crystallized at 41 °C. Cross-polarized optical micrographs describing the extinction rings of (f) PCL/MMT, (g) 1 wt% PVB2 in PCL/PVB2/MMT, (h) 5 wt% PVB2 in PCL/PVB2/MMT and (i) 10 wt% PVB2 in PCL/PVB2/MMT spherulites without CB crystallized at 41 °C, (j) Cross-polarized optical micrographs of 5 wt% PVB2 in PCL/PVB/MMT with CB crystallized at 41 °C.

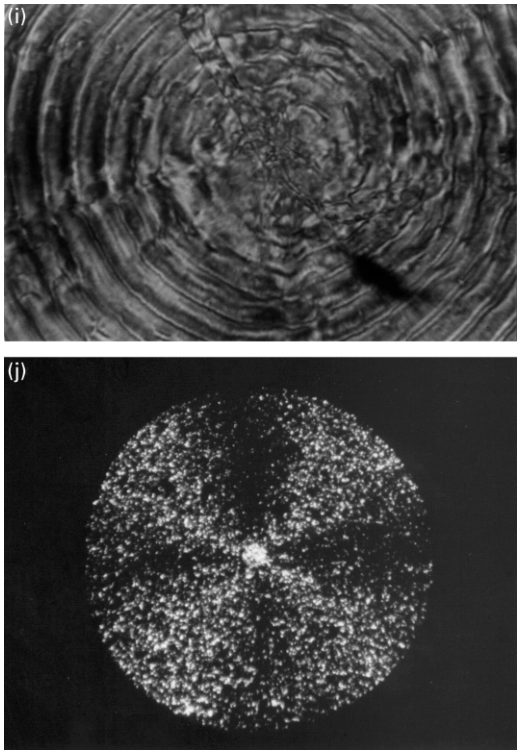

Fig. 2 (*continued*)

nucleation density obtained in PCL/PVB2 with CB is similar to the observation of the system without CB. The growth front of the spherulite was also clearly observed with CB. Therefore the spherulite growth rate can be estimated by these microscopic observations during isothermal crystallization. Similar banding structure is also obtained for PCL/PVB1 and PCL/PVB3 systems, but the banding spacings of PCL/PVB polymer blend slightly decrease as the molecular weight of PVB increases. Its occurrence implies a short period of PCL lamellar twisting as the molecular weight of PVB increases.

For PCL/PVB2/MMT system, the effect of MMT on the crystallization behavior and morphology of PCL/PVB2 is also shown in Fig. 2. Addition of CTAB-modified MMT into PCL, the grown spherulites crystallized from the melt show similar extinction crosses as those observed for pure PCL. The addition of MMT into PCL/PVB2, all POM data show the decreasing nucleation density in PCL/PVB2 with the presence of small amount of dispersed MMT. The spherulites grown in PCL/PVB2/MMT also exhibit banding with small radial separations, but the band spacings are decreased with increasing PVB2 content and the addition of MMT. This result indicates that increasing the PVB2 content and addition of MMT shortens the period of lamellar twisting. The band spacings are further decreased at the same PVB2 content in PCL/PVB2/MMT compared to PCL/PVB2, and this indicates that the addition of MMT can further reduce the period of lamellar twisting. Addition of CB into PCL/PVB2/MMT system also show unclear boundary of spherulite. Larger spherulite with a Maltese cross in PCL/PVB2/MMT was observed even though the presence of poor visual field with CB. The nucleation density in PCL/PVB2/MMT with CB is similar to the observation of the system without CB and the growth front of the spherulite was clearly observed with the presence of CB. These results of microscopic observations during isothermal crystallization were also used to estimate the spherulite growth rate. Similar banding structure is obtained for PCL/PVB1/MMT and PCL/PVB3/MMT systems, but the banding spacings of PCL/PVB/MMT nanocomposites slightly decrease as the molecular weight of PVB increases. Its occurrence implies a short period of PCL lamellar twisting as the molecular weight of PVB increases.

Fig. 3 shows the PVB2 content dependence on the growth rate (G) of the spherulites in PCL/PVB2 and PCL/PVB2/MMT systems with and without CB. An almost straight line was obtained for each sample in PCL/PVB2 and PCL/PVB2/MMT systems, and the growth rate $G = \mathrm{d}R/\mathrm{d}t$ (R denotes the radius of a spherulite) was determined from the slope of each line. Growth rates are smaller in the PCL/PVB2 compared to pure PCL and decrease with increasing the content of PVB2 but only by a factor about 1.5–3 in growth at 41 °C for 10 wt% PVB2, while CB has little effect on the nucleation of PCL or the growth rate of spherulites. This result is not inordinate in comparison with what is commonly observed in crystalline polymers containing amorphous PVB. The growth rates are further increased at the same PVB2 content in PCL/PVB2/MMT

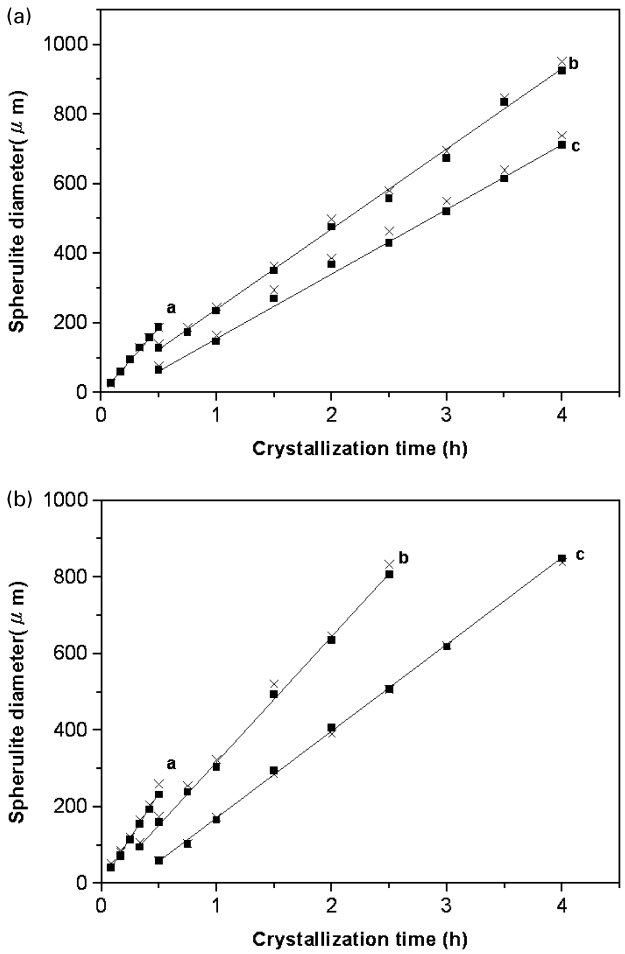

Fig. 3. (a) Size of spherulites versus crystallization time for PCL/PVB2 with (a) 1 wt% PVB2, (b) 5 wt% PVB2 and (c) 10 wt% PVB2. All results are crystallized at 41 °C. Solid (●) symbols denote the samples containing 5 wt% CB; (×) symbols denote those without CB. (b) Size of spherulites versus crystallization time for PCL/PVB2/MMT with (a) 1 wt% PVB2, (b) 5 wt% PVB2 and (c) 10 wt% PVB2. All results are crystallized at 41 °C. Solid (●) symbols denote the samples containing 5 wt% CB; (×) symbols denote those without CB.

nanocomposites compared to PCL/PVB2, indicating that the addition of MMT can further accelerate the formation of PCL spherulites. These observations showed the crystallization of the PCL/PVB2/MMT is retarded by the addition of PVB2, while CB has little effect on the nucleation of PCL or the spherulite growth rate. At the same time, the addition of 1 wt% MMT into PCL can accelerate the formation of PCL spherulites and then decrease the nucleation density of PCL crystalline. Similar results are also reported for polyamide/clay and sPS/clay nanocomposites with small content of MMT [26–28], indicating that formation of crystal growth is dominant as the addition of small amount of MMT. The crystal formation for PCL/PVB1/MMT and PCL/PVB3/MMT systems is similar to that observed for PCL/PVB3/MMT system, but the growth rates of PCL/PVB/MMT nanocomposites is almost independent of the molecular weight of PVB. Detailed analysis of crystallization kinetics and melting behaviors of PCL/PVB/MMT nanocomposites by well-known Avrami equation would be discussed below.

The spherulitic morphologies and nucleation mechanism in PCL/PVB/MMT nanocomposites can be determined by applying the isothermal crystallization to these specimens at $T_c = 41$ °C. The overall crystallization kinetics of PCL/PVB/MMT nanocomposites can be correlated by Avrami equation [29]:

$$1 - X_t = \exp(-k(t_f - t_{start})^n) \quad (1)$$

where X_t is the time-dependent volume fraction crystallinity, k is the crystallization constant (min^{-1}), t_{start} is the initial time of crystallization (min), t_f is the time elapsed (min) and n is the Avrami exponent. Eq. (1) can be transformed into

$$\ln[-\ln(1 - X_t)] = n \ln(t - t_{start}) + \ln k \quad (2)$$

The Avrami exponent n is recognized that can provide possible spherulitic morphologies and nucleation mechanism related to the type of nucleation and the geometry of the growing crystals. Fig. 4 show the plots of $ln[-\ln(1 - X_t)]$ versus $\ln(t - t_{start})$ for PCL/PVB/MMT nanocomposites. As predicted by the equation, a linear portion in the development of crystallinity is observed in each plot of $\ln[-\ln(1 - X_t)]$ versus $\ln(t - t_{start})$ with slope n and intercept $\log k$. The plots of $\ln[-\ln(1 - X_t)]$ versus $\ln(t - t_{start})$ for various molecular weight of PVB in PCL/PVB/MMT nanocomposites show similar linear tendency and the crystallization parameters ΔH_0, t_{start}, k, and n are summarized in Table 1.

As pure PCL was isothermally crystallized at 41 °C, the n value is close to 3.0, representing an athermal nucleation process followed by a three-dimensional crystal growth is also consistent with the spherulitic observation by POM. The n values of PCL/PVB and PCL/PVB/MMT are smaller than that of PCL. The addition of 1 wt% amorphous PVB2 into PCL, the n value is decreased with the presence of small

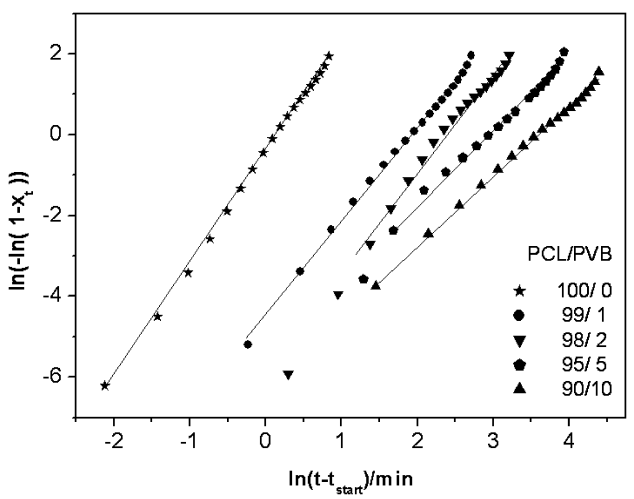

Fig. 4. Plots of $\ln[-\ln(1 - X_t)]$ versus $\ln(t - t_{start})$ for PCL/PVB2/MMT nanocomposites.

Table 1
Avrami exponents at $T_c = 41$ °C for isothermal crystallization of PCL/PVB/MMT nanocomposites

Specimen	t_{start} (min)	ΔH_0 (J/g)	n	k ($\times 10^4$)	$t_{1/2}$
PCL	0.69	47.92	2.90	15,200	1.02
PCL/PVB1 (1 wt%)	1.51	52.52	2.89	30.8	6.48
PCL/PVB1 (5 wt%)	4.04	45.73	2.69	1.91	20.6
PCL/PVB1 (10 wt%)	26.2	23.88	2.60	0.46	40.2
PCL/PVB2 (1 wt%)	0.77	46.56	2.84	636	8.47
PCL/PVB2 (5 wt%)	4.55	45.11	2.60	1.32	33.9
PCL/PVB2 (10 wt%)	44.3	19.8	2.41	0.49	55.9
PCL/PVB3 (1 wt%)	0.81	47.19	2.70	12,400	13.3
PCL/PVB3 (5 wt%)	9.04	46.93	2.29	0.85	54.9
PCL/PVB3 (10 wt%)	56.8	16.76	2.00	0.47	77.9
PCL/MMT	0.65	46.30	3.02	19400	0.81
PCL/PVB1 (1 wt%)/MMT	0.85	51.05	2.75	4700	0.96
PCL/PVB1 (5 wt%)/MMT	2.88	46.50	2.54	7.69	14.2
PCL/PVB1 (10 wt%)/MMT	7.03	15.05	2.58	2.60	20.3
PCL/PVB2 (1 wt%)/MMT	0.85	52.90	2.60	890	0.94
PCL/PVB2 (5 wt%)/MMT	2.88	46.38	2.48	121	14.9
PCL/PVB2 (10 wt%)/MMT	7.11	16.02	2.41	16.9	23.5
PCL/PVB3 (1 wt%)/MMT	0.82	59.79	2.32	117	0.97
PCL/PVB3 (5 wt%)/MMT	2.75	45.36	1.79	53.5	15.2
PCL/PVB3 (10 wt%)/MMT	7.42	16.25	1.71	21.5	28.3

amount of PVB2. The addition of more PVB2 into PCL, the n values further decrease and range from 2.6 to around 2.4 with increasing the content of PVB2. The value of $n \approx 2.0$ indicates that crystal growth may not occur in three dimensions at an equal rate and hence a low n value is obtained. The non-integral n values we obtained might be due to the presence of crystalline branching and/or two stage crystal growth during the crystallization process and/or mixed growth and nucleation mechanism [30]. Therefore this results indicate that introducing a small amount of amorphous PVB into the PCL structure causes a change of the crystal growth process from a three dimensional to a mixed three-dimensional and two-dimensional spherulitic growth. Similar mechanism of crystal growth is also obtained for PCL/PVB1 and PCL/PVB3 systems, but the n value of PCL/PVB slightly decrease as the molecular weight of PVB increases. Its occurrence implies a high amount of two-dimensional crystal growth occurs as the molecular weight of PVB increases and the addition of MMT. Addition of CTAB-modified MMT into PCL/PVB, the grown spherulites represented by n values in the range of 2.4–2.6 are an athermal nucleation process followed by a mixed three-dimensional and two-dimensional spherulitic growth. At the same PVB2 content in PCL/PVB/MMT compared to PCL/PVB, the n values are further decreased, and this indicate that the addition of MMT also change the mechanism of crystal growth. Similar behavior of crystal growth is also observed for PCL/PVB1/MMT and PCL/PVB3/MMT systems, but the n value of PCL/PVB/MMT nanocomposite decrease to the range of 1.7–2.3 as the molecular weight of PVB increases. Its occurrence implies a high amount of two-dimensional crystal growth occurs as the molecular weight of PVB increases and the addition of MMT. Therefore the high molecular weight of PVB and the addition of MMT favor the formation of two-dimensional crystal growth.

From above results, the growth rate should decrease during crystallization due to the increase of the diluent concentration at the growth front if an amorphous is rejected by the growing lamellae of crystalline. As the spherulites grow, the diluent concentration increases rapidly around the impinging spherulites. This causes a marked reduction in the growth rate and flattening of the round spherulite profile. However, such flattening was not observed in this study. This implies that the concentration of the crystallizable PCL component at the growing front remains constant throughout the spherulite growth. That is probably due to the presence of a polar interaction and/or hydrogen bonding between C=O in PCL and OH function group in PVB prevents strong segregation of PVB. Therefore, PVB is not expelled from the spherulites and remains mainly in the amorphous region between the PCL lamellae. Similar observations are also obtained for PCL/PVB/MMT nanocomposites. The addition of nanoscale MMT has little effect on the morphology of PCL spherulites. Although these observations gave us a very important insight into the crystallization behavior and morphology of PCL/PVB and PCL/PVB/MMT materials, we still obtained no information on the distribution of CB in the spherulites because the size of CB is too small to be observed by optical microscopy. Nevertheless, these results indicate that the PCL/PVB/MMT nanocomposites are probably suitable for studying the effect of morphological changes on the PTC properties due to the presence of possibly remarkable change in the morphology of the PCL/PVB/MMT as those observed for PCL/PVB materials.

Fig. 5 shows the temperature dependence of the resistivity ρ and DSC melting curve of pure PCL with 5 wt% CB and 5 wt% PVB2 in PCL/PVB2 and PCL/PVB2/MMT with 5 wt% CB. The resistivity-temperature curves slightly shifted

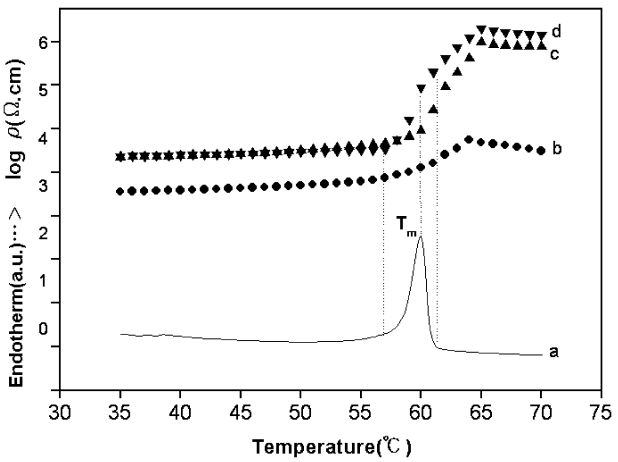

Fig. 5. (a) DSC melting curve of pure PCL with 5 wt% CB, (b) temperature dependence of the resistivity ρ for pure PCL with 5 wt% CB, (c) temperature dependence of the resistivity ρ for 5 wt% PVB2 in PCL/PVB2 with 5 wt% CB and (d) temperature dependence of the resistivity ρ for 5 wt% PVB2 in PCL/PVB2/MMT with 5 wt% CB.

upward with the presence of PVB2 and the PTC intensity I_{PTC}, defined as the resistivity ratio ρ_{max}/ρ_{min}, was also increased. Here ρ_{max} is the maximum value of the curve and ρ_{min} is the resistivity at room temperature. For 5 wt% PVB in PCL/PVB2/MMT, the I_{PTC} further increased with the addition of MMT. The resistivity started to increase when the lamellar crystals began to melt and abruptly increased when the temperature approached $T_{max,\ DSC}$. It reached the maximum around $T_{max,\ DSC}$ and started to decrease gradually after that temperature as a result of the reagglomerization of CB particles in the molten polymer phase (negative temperature coefficient (NTC)). Thus the resistivity change is strongly related to the melting process and the morphology of materials. These results also indicate that the drastic PTC property change originates from the abrupt volume expansion of melting lamellae displaced CB. Therefore it changes the distribution of interparticle gaps and the resistivity of PTC materials. According to previous models, a conductive path is probably along a crystalline lamellae or a fibril in a spherulite. When the PCL crystalline lamellae melt, they change the interparticle gap width and make the distribution more random. Most of the CB particles in PCL/PVB and PCL/PVB/MMT systems move perpendicularly to the surface of a non-twisted lamellae, while CB close to a twisted lamellae moves in almost all directions. Increasing the PVB content reduces the period of the lamellae twist; this increases the displacement of the CB near the lamella surface. Similar I_{PTC} effect on the PVB content is also observed for PCL/PVB1, PCL/PVB3, PCL/PVB1/MMT and PCL/PVB3/MMT systems. The resistivity-temperature relation of PCL/PVB and PCL/PVB/MMT systems increases as the molecular weight of PVB increases.

Fig. 6 shows the effect of the content of CB on the PTC properties of 5 wt% PVB2 in PCL/PVB2 and PCL/PVB2/MMT systems. The I_{PTC} increased with the CB ratio up to 5 wt% and then gradually decreased with the CB ratio to 10 wt%. At least three specimens for a given CB ratio were measured. Therefore 5% CB were used for the following PCL/PVB2 and PCL/PVB2/MMT preparations. Fig. 7 shows the effect of PVB2 ratio on the PTC properties of PCL/PVB2 and PCL/PVB2/MMT systems containing 5 wt% CB. By adding as small as 2 wt% PVB2 into PCL, I_{PTC} increased more than 5 times than that of PCL. The addition of MMT can further improve the thermoelectric properties of PTC materials by a factor about 1.5–2. Surprisingly, I_{PTC} of the nanocomposites with 5 wt% PVB2 was larger than that of PCL/MMT by almost fifteen times of magnitude. It is necessary to note that the amount of these nanocomposites had the same amount of CB, and the difference was only in the PVB2 concentration. Similar I_{PTC} increased with the PVB content are also shown in Table 2 for PCL/PVB and PCL/PVB/MMT systems.

Fig. 8 shows the X-ray data of various PVB2 content in PCL/PVB2/MMT nanocomposites with 5 wt% CB. All results show a similar X-ray pattern, indicating that the addition of amorphous PVB2 into crystalline PCL with the presence of MMT and CB does not significantly change the crystalline structure of PCL. The crystallinity of specimen was obtained

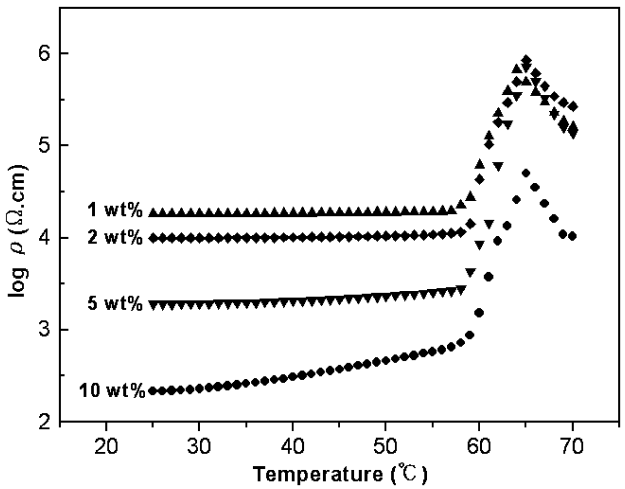

Fig. 6. Effect of the content of CB on the PTC properties of PCL/PVB2/MMT nanocomposites.

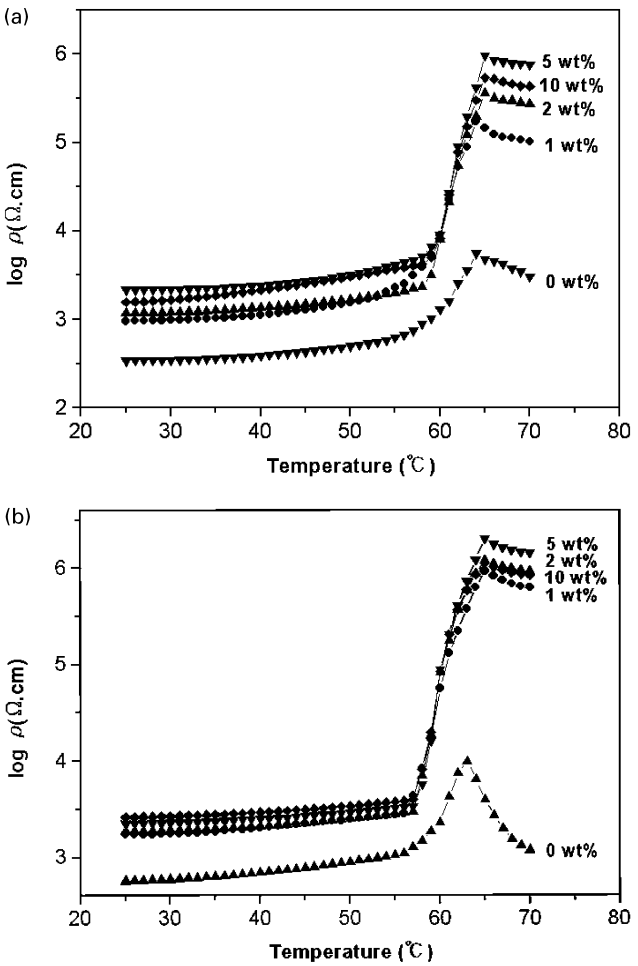

Fig. 7. Effect of PVB2 ratio on the PTC properties of PCL/PVB2/MMT nanocomposites containing 5 wt% CB.

Table 2
PTC intensity of PCL/PVB/MMT nanocomposites

Specimen	I_{PTC}
PCL	12.9
PCL/PVB1 (1 wt%)	243
PCL/PVB1 (5 wt%)	378
PCL/PVB1 (10 wt%)	176
PCL/PVB2 (1 wt%)	255
PCL/PVB2 (5 wt%)	378
PCL/PVB2 (10 wt%)	190
PCL/PVB3 (1 wt%)	285
PCL/PVB3 (5 wt%)	427
PCL/PVB3 (10 wt%)	330
PCL/MMT	18.4
PCL/PVB1 (1 wt%)/MMT	345
PCL/PVB1 (5 wt%)/MMT	593
PCL/PVB1 (10 wt%)/MMT	194
PCL/PVB2 (1 wt%)/MMT	456
PCL/PVB2 (5 wt%)/MMT	721
PCL/PVB2 (10 wt%)/MMT	278
PCL/PVB3 (1 wt%)/MMT	535
PCL/PVB3 (5 wt%)/MMT	898
PCL/PVB3 (10 wt%)/MMT	433

by the curve fitting to calculate the area of each peak. A linear background correction was applied separately to the observed peaks before to obtain the area of each peak, for which we assumed Gaussian profiles. The calculated crystallinity of various PVB2 content in PCL/PVB2/MMT nanocomposites showed no noticeable change for at least 10 wt% PVB2. This result indicates that drastic changes in PTC properties do not come from the changes in crystalline properties of PCL, but from the morphology of PCL spherulite.

From above results, the increasing PVB concentration in PCL/PVB/MMT nanocomposites drastically decreased the band spacing, whereas I_{PTC} increased. The influence of MMT on the I_{PTC} was less profound than that of PVB concentration, but the presence of MMT can further improve thermoelectric properties of PTC materials by a factor about 1.5–2. At the same time, the crystallinity of specimens remains almost unchanged. Therefore these results indicate that increasing PVB content and addition of MMT can shorten the period of lamellae twisting and causes shorter interparticle gap and more complex displacement of CB in the melting process.

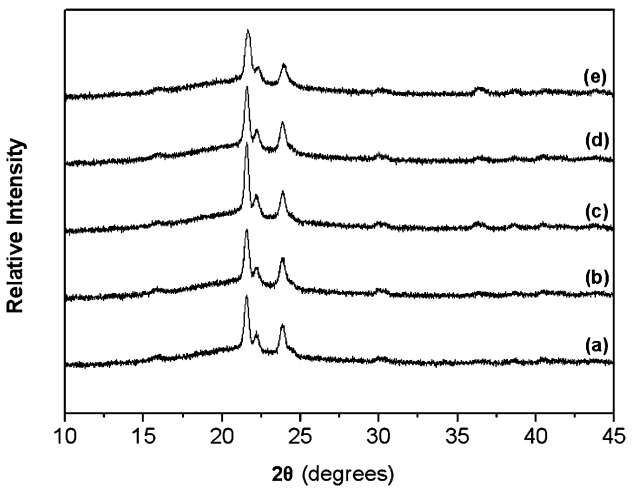

Fig. 8. X-ray data of with (a) pure PCL/MMT2, (b) 1 wt% PVB, (c) 2 wt%, (d) 5 wt% PVB2 and (e) 10 wt% PVB2 content in PCL/PVB2/MMT nanocomposites with 5 wt% CB.

4. Conclusions

The band spacings of PCL spherulites in PCL/PVB/MMT nanocomposites decrease with increasing PVB content and the presence of 1 wt% MMT, and this indicates that increasing the PVB content and 1 wt% MMT addition can shorten the period of lamellar twisting. The increasing molecular weight of PVB also causes the decrease of the period of crystalline PCL lamellar twisting, but the influence of molecular weight on the band spacing is less profound than that of PVB concentration. The intensity of PTC of the nanocomposites was increased as the band spacings decrease. These results indicate that the increasing PVB content and the molecular weight of PVB can shorten the period of lamellae twisting and causes shorter interparticle gap between CB in the melting process.

Acknowledgements

The financial support provided by NSC through the project NSC90-2216-E-005-026 was greatly appreciated.

References

[1] Narkis M, Ram A, Flashner F. Polym Engng Sci 1978;18:649.
[2] Yu G, Zhang MQ, Zeng HM. J Appl Polym Sci 1998;70:559.
[3] Yi X-S, Wu G, Ma D. J Appl Polym Sci 1998;67:131.
[4] Knackstedt MA, Roberts AP. Macromolecules 1996;29:1369.
[5] Sumita M, Sakata K, Hayakawa Y, Asai S, Miyasaka K, Tanemura M. Colloid Polym Sci 1992;270:134.
[6] Al-Allak HM, Brinkman AW, Woods J. J Mater Sci 1993;28:117.
[7] Zhang MQ, Yu G, Zeng HM, Zhang HB, Hou YH. Macromolecules 1998;31:6724.
[8] Wang B, Yi X, Pan Y, Shan HJ. Mater Sci Lett 1997;16:2005.
[9] Sumita M, Sakata K, Asai S, Miyasaka K, Nakagawa H. Polym Bull 1991;25:265.
[10] Gubbles E, Blacher S, Vanlathem E, Jerome R, Deltour R, Brouers F, Teyssle Ph. Macromolecules 1995;28:1559.
[11] Meyer J. Polym Engng Sci 1974;14:706.
[12] Kohler FUS. Patent 3,243,753 March 29; 1966.
[13] Ohe K, Natio Y. Jpn J Appl Phys 1971;10:99.
[14] Sumita M, Sakata K, Asai S, Miyasaka K, Nakagawa H. Polym Bull 1991;25:265.
[15] Reghu M, Yoon C, Yang C, Moses D, Heeger A, Cao Y. Macromolecules 1993;26:7245.
[16] Gubbles F, Jerome R, Teyssie P, Vanlathem E, Deltour R, Calderone A, Parente V, Bredas J. Macromolecules 1994;27:1972.

[17] Knackstedt MA, Roberts AP. Macromolecules 1996;29:1369.
[18] Sherman RD, Middleman LM, Jacobsa SM. Polym Engng Sci 1983; 23:36.
[19] Keith HD, Padden JrFJ, Russel TP. Macromolecules 1989;22:666.
[20] Lee J-C, Nakajima K, Ikehara T, Nishi T. J Appl Polym Sci 1997;65: 409.
[21] Lee J-C, Ikehara T, Nishi T. J Appl Polym Sci 1998;69:193.
[22] Ozin GA. Adv Mater 1992;4:612–45.
[23] Novak BM. Adv Mater 1993;5:422–33.
[24] Kojima Y, Usuki A, Kawasumi M, Okada A, Kurauchi T, Kamigaito O, Kaji K. J Polym Sci, Part B: Polym Phys 1988;26:1947.
[25] Hulteen JC, Martin CR. J Mater Chem 1997;7:1075.
[26] Wu T-M, Liao C-S. Macromol Chem Phys 2000;201:2820.
[27] Wu T-M, Wu J-Y. J Macromol Sci Phys 2002;41:17.
[28] Wu T-M, Hsu S-F, Wu J-Y. J Polym Sci, Part B: Polym Phys 2002;40: 736.
[29] Avrami M. J Chem Phys 1939;7:1103.
[30] Alamo RG, Mandelkern L. Macromolecules 1991;24:6480.